Anal. Chem. **2010,** *82,* 5147–5153

Three-Dimensionally Assembled Gold Nanostructures for Plasmonic Biosensors

Longhua Guo,[†] Guonan Chen,[‡] and Dong-Hwan Kim*,[†]

School of Chemical and Biomedical Engineering, Nanyang Technological University, 70 Nanyang Drive, Singapore 637457, Singapore, and Ministry of Education Key Laboratory of Analysis and Detection Technology for Food Safety, Department of Chemistry, Fuzhou University, Fuzhou 350002, China

Three-dimensional gold nanoarchitecture was fabricated by layer-by-layer (LbL) deposition of gold nanoparticles (AuNPs) and multiwalled carbon nanotubes (MWCNTs) on a glass substrate for a highly sensitive plasmonic biosensor using a conventional UV−vis instrument. Carboxyl-functionalized MWCNTs were reacted with 3-mercaptopropyltriethoxysilane (MPTES) to introduce multiple thiol groups onto MWCNTs. A self-assembled monolayer (SAM) of AuNPs on a glass chip was sequentially dipped into MPTES-functionalized MWCNTs (MWCNT-Si-SH) and AuNPs to form multilayers of AuNPs on MWCNTs. Such three-dimensionally assembled AuNPs provided a large surface area and multiple binding sites within a few steps of modification and microporous structures of multilayered MWCNTs to allow a high accessibility of target molecules. It was shown that the bulk refractive index (RI) sensitivity of these multilayered AuNPs (three-dimensional chip) appeared to be 5.6 times better than that of a monolayer of AuNPs on a glass chip (two-dimensional chip). The three-dimensional chips were further used for a biomolecular binding study, showing a detection limit as low as 0.5 nM for streptavidin and 3.33 nM for anti-human serum albumin (HSA), both of which were ∼20 times higher than the sensitivity of the two-dimensional chips.

The phenomenon of localized surface plasmon resonance (LSPR), which results from the plasmonic response of noble nanometallic particles to incident electromagnetic waves,[1] can be exploited in the label-free sensing of analytes and also in devices such as nanoscale biosensors.[2−4] Binding of analytes on metallic surfaces causes a change in the local refractive indices (RIs) of the surrounding dielectric, resulting in either a shift in the spectral extinction peak or a change in the peak intensity. Transmission spectrometry, which is relatively simple and inexpensive, can be used for LSPR sensing of 10−100 nm particles in the UV−vis region,[5−7] whereas conventional SPR operates in total internal reflection mode, thus requiring a sophisticated detection system. In addition to LSPR's superiority to SPR, the strong demand for rapid, cost-effective, and high-throughput measurements has led to the development of a chip-based assay consisting of metal nanoparticles immobilized on a substrate.[8−13] However, the fabrication of nanostructured LSPR sensors that are sensitive to a conventional UV−vis instrument is still a challenging task mainly because LSPR signals are often weak because of the low density of nanoparticles in the defined surface area. Herein, we report on the fabrication of a three-dimensional structure of AuNPs constructed on carbon nanotube (CNT) templates for a highly sensitive plasmonic biosensor using a conventional UV−vis instrument.

Various strategies, including nanoparticle design, nanofabrication techniques,[14−16] and improvement of instrumental resolution,[17] have been introduced to achieve highly sensitive molecular detection. The feasibility of single-molecule detection has recently been demonstrated.[7,18] Since the introduction of chip-based assays using nanoparticles immobilized on a transparent substrate,[9] most subsequent research has focused on the application of a monolayer of nanoparticles on a solid support, a so-called two-dimensional (2D) chip.[8−10] However, the sensitivity of 2D chips under conventional UV−vis instruments is confined by the limited

* To whom correspondence should be addressed. E-mail: dhkim@ntu.edu.sg. Fax: 65-67911761.

† Nanyang Technological University.

‡ Fuzhou University.

(1) Bohren, C. F.; Huffman, D. R. *Absorption and scattering of light by small particles*; Wiley-Interscience: New York, 1983.
(2) Hutter, E.; Fendler, J. *Adv. Mater.* **2004**, *16*, 1685–1706.
(3) Daniel, M.; Astruc, D. *Chem. Rev.* **2004**, *104*, 293–346.
(4) Haes, A. J.; Duyne, R. P. V. *Expert Rev. Mol. Diagn.* **2004**, *4*, 527–537.
(5) Anker, J. N.; Hall, W. P.; Lyandres, O.; Shah, N. C.; Zhao, J.; Van Duyne, R. P. *Nat. Mater.* **2008**, *7*, 442–453.
(6) Willets, K. A.; Van Duyne, R. P. *Annu. Rev. Phys. Chem.* **2007**, *58*, 267–297.
(7) Nusz, G.; Curry, A.; Marinakos, S.; Wax, A.; Chilkoti, A. *ACS Nano* **2009**, *3*, 795–806.
(8) Malinsky, M. D.; Kelly, K. L.; Schatz, G. C.; Van Duyne, R. P. *J. Am. Chem. Soc.* **2001**, *123*, 1471–1482.
(9) Nath, N.; Chilkoti, A. *Anal. Chem.* **2002**, *74*, 504–509.
(10) Nath, N.; Chilkoti, A. *Anal. Chem.* **2004**, *76*, 5370–5378.
(11) Kreuzer, M. P.; Quidant, R.; Salvador, J. P.; Marco, M. P.; Badenes, G. *Anal. Bioanal. Chem.* **2008**, *391*, 1813–1820.
(12) Huang, H.; He, C.; Zeng, Y.; Xia, X.; Yu, X.; Yi, P.; Chen, Z. *Biosens. Bioelectron.* **2009**, *24*, 2255–2259.
(13) Kim, D. K.; Kerman, K.; Saito, M.; Sathuluri, R. R.; Endo, T.; Yamamura, S.; Kwon, Y. S.; Tamiya, E. *Anal. Chem.* **2007**, *79*, 1855–1864.
(14) Aslan, K.; Lakowicz, J. R.; Szmacinski, H.; Geddes, C. D. *J. Fluoresc.* **2005**, *15*, 37–40.
(15) Haes, A. J.; Zou, S.; Schatz, G. C.; Van Duyne, R. P. *J. Phys. Chem. B* **2004**, *108*, 6961–6968.
(16) Hicks, E. M.; Zhang, X.; Zou, S.; Lyandres, O.; Spears, K. G.; Schatz, G. C.; Van Duyne, R. P. *J. Phys. Chem. B* **2005**, *109*, 22351–22358.
(17) Dahlin, A. B.; Tegenfeldt, J. O.; Hook, F. *Anal. Chem.* **2006**, *78*, 4416–4423.
(18) Huang, T.; Nallathamby, P. D.; Xu, X. H. *J. Am. Chem. Soc.* **2008**, *130*, 17095–17105.

10.1021/ac100346z
Published on Web 05/14/2010

density of nanoparticles on a substrate. To the best of our knowledge, there have been only a few attempts to create three-dimensional (3D) LSPR structures to increase the nanoparticle ensemble density.[19−23] Gu and co-workers[19,20] developed a metal-coated macroporous film using silica spheres. They have shown that both the LSPR of the metal nanoparticles and the stop band of the silica spheres could be used to measure the binding events of biomolecules. Ye et al.[21] reported a simple strategy for fabricating multilayers of AuNPs on a glass surface by alternating the deposition of bifunctional cross-linkers and AuNPs; this approach showed enhanced sensitivity compared to a monolayer of AuNPs. However, the tiny space between the layers of AuNPs keeps target molecules from binding to their receptors that reside below the surface of the AuNP structures. This motivated us to create highly accessible AuNP structures that provide high ensemble density and offer sufficient room for the diffusion of target molecules within AuNPs layers.

CNT−metallic nanoparticle composites were introduced for use in heterogeneous catalysis[24] and hydrogen sensing.[25] Despite their potential applications in biomolecule detection, until now there have been no reports of metal nanoparticle-decorated CNTs for LSPR-based biosensors. Here, we present a novel strategy for fabricating high-density, multilayered AuNPs on MWCNT templates using LbL deposition (namely, 3D chips). MWCNT was used as a framework for AuNP assembly because of its unique characteristics. First, MWCNT possesses a large surface area and multiple binding sites. Second, the multiple layers of MWCNT would have microporous structure that could allow biomolecules to diffuse into the inner layers of the MWCNT. 3-Mercaptopropyltriethoxysilane (MPTES) was used to functionalize MWCNT for the first time. Conventional aliphatic bifunctional thiols provide only one SH group. On the other hand, the thiol-silane introduces multiple SH groups into each binding site of MWCNTs because of its self-polymerization capability, thus allowing high-density AuNPs on the MWCNT template.

EXPERIMENTAL SECTION

AuNP Synthesis. Gold nanospheres (13 nm) were prepared by sodium citrate reduction of $HAuCl_4 \cdot 3H_2O$ as described previously, with slight modifications.[26,27] All glassware used for AuNPs preparation was thoroughly washed with aqua regia (3:1 HCl/HNO_3), rinsed extensively with distilled water, and then dried in an oven at 100 °C for at least 1 h. Forty microliters of 2.5 M $HAuCl_4$ and 100 mL of Millipore water were added to a two-neck flask. After the condenser had been connected to one neck of the flask and a stopper placed in the other neck, the flask was placed on the hot plate to reflux with stirring. When the solution began to reflux, the stopper was removed. Then, 10 mL of 38.8 mM sodium citrate was quickly added and the stopper was put back in place. After being refluxed for an additional 20 min, the system was allowed to cool to room temperature while being stirred. The AuNPs were then filtered with 0.45 μm acetate filters and stored at room temperature.

UV−Vis Measurements. All absorption spectra were recorded with a Shimadzu UV-2450 spectrophotometer in transmission mode. A rectangular quartz cell with dimensions of 20 mm (length) × 2 mm (width) × 20 mm (height) was designed in house to hold the glass chips.

Bulk Solution Refractive Index Study. RI studies were performed by immersing the 2D/3D chips in water (n = 1.333), ethanol (n = 1.36), butanol (n = 1.396), dimethylformamide (n = 1.431), and dimethyl sulfoxide (n = 1.478). The extinction spectra were recorded with a Shimadzu UV-2450 spectrophotometer.

Microscopy. FE-SEM was performed on the JEOL instrument (JSM-6700F) at an acceleration voltage of 5 kV and a working distance of 7−8 mm. Samples on glass chips were coated with Pt for 30−60 s at 20 mA, whereas samples on silicon wafers were observed under FE-SEM without a Pt coating.

Functionalization of MWCNTs. MWCNT-COOH [outside diameter of 20−30 nm, inside diameter of 5−10 nm, length of 10−30 μm, 1.23% COOH (m/m)] was purchased from Chendu Organic Chemistry Co. Ltd., Chinese Academy of Sciences. Purification was performed via sonication in 5 M HCl for 4 h at room temperature to remove metal catalysts. The purified MWCNT-COOH was filtered, washed with deionized water until the pH reached 7, and dried in a vacuum. Then, 15 mg of MWCNT-COOH was left to react with 30 mL of 10% MPTES in ethanol and refluxed for 3 h under constant stirring and with the temperature maintained at ∼70 °C. The entire reaction was conducted in a nitrogen atmosphere to prevent the oxidation of SH. The MWCNT-Si-SH was centrifuged at 4500 rpm for 15 min, washed with ethanol three times to remove the excess MPTES, and vacuum-dried at 60 °C for 3 h.

Fabrication of the 3D Chip. Figure 1 shows the steps for the fabrication of the 3D chip. The detailed procedures are as described below. (1) Microscope coverslips (18 mm × 18 mm, No. 1.5, Thermo Fisher Scientific Inc.) were cleaned in a "piranha" bath (30% H_2O_2 mixed in a 1:4 ratio with concentrated H_2SO_4) at 60 °C for 15 min and then thoroughly rinsed with water and ethanol. (2) The slides were incubated in a 10% solution of APTES in ethanol for 2 h, resulting in the formation of an amino-terminated, self-assembled silane monolayer (SAM) on the glass surface. The cover glass was then washed with ethanol, sonicated in ethanol three times for 3 min each, and then dried at 120 °C for 2 h. (3) The silanized glass coverslips were subsequently immersed in a AuNP solution (∼13 nM) for 2 h to form a self-assembled monolayer of AuNPs on both sides of the glass (2D chip). (4) The 2D chips were then modified with MWCNT by immersion in a 0.1 mg/mL solution of MWCNT-Si-SH in dimethylformamide (DMF) for 3 h under constant stirring. The chips were picked out, rinsed with deionized water, and dried with a nitrogen stream. (5) The chips were immersed in the AuNP solution again for 2 h to immobilize the AuNPs onto the MWCNTs. The chips were then

(19) Chen, H. H.; Suzuki, H.; Sato, O.; Gu, Z. Z. *Appl. Phys. A: Mater. Sci. Process.* **2005**, *81*, 1127–1130.
(20) Gu, Z. Z.; Horie, R.; Kubo, S.; Yamada, Y.; Fujishima, A.; Sato, O. *Angew. Chem., Int. Ed.* **2002**, *41*, 1153–1156.
(21) Ye, J.; Bonroy, K.; Nelis, D.; Frederix, F.; D'Haen, J.; Maes, G.; Borghs, G. *Colloids Surf., A* **2008**, *321*, 313–317.
(22) Lu, Y.; Wang, Q.; Sun, J.; Shen, J. *Langmuir* **2005**, *21*, 5179–5184.
(23) Jiang, C.; Markutsya, S.; TsukrukMalikova, V. V. *Langmuir* **2004**, *20*, 882–890.
(24) Che, G.; Lakshmi, B.; Fisher, E.; Martin, C. *Nature* **1998**, *393*, 346–349.
(25) Kong, J.; Chapline, M.; Dai, H. *Appl. Phys. Lett.* **1995**, *66*, 159.
(26) Frens, G. *Nature (London), Phys. Sci.* **1973**, *241*, 20–22.
(27) Liu, J.; Lu, Y. *Nat. Protoc.* **2006**, *1*, 246–252.

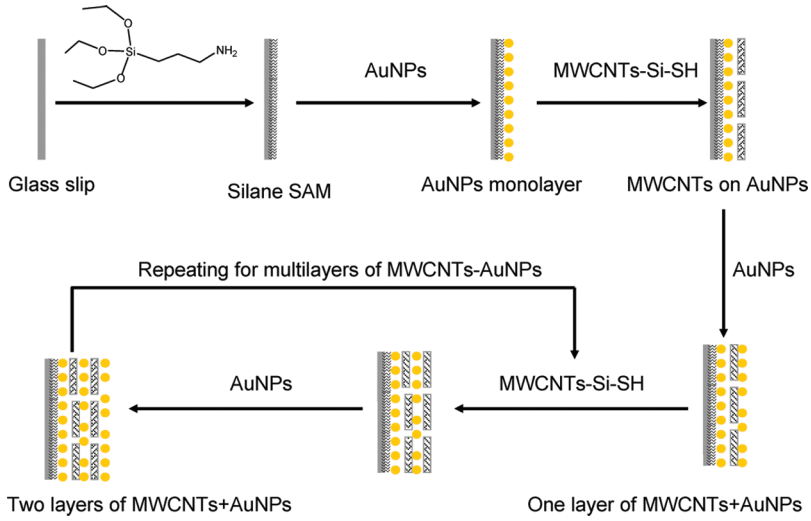

Figure 1. Schematic of the steps involved in the fabrication of the 3D AuNP biosensor on a glass surface.

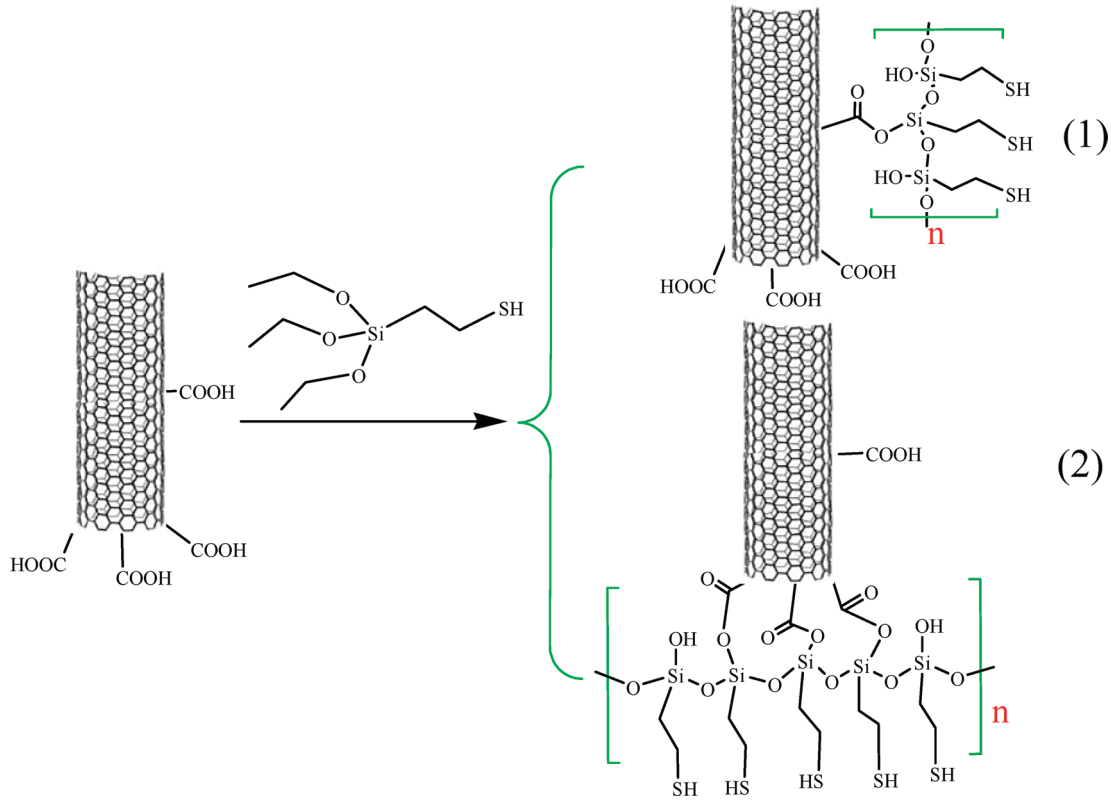

Figure 2. Schematic diagram of MWCNTs functionalized with MPTES.

rinsed with deionized water and dried with nitrogen. (6) Steps 4 and 5 were repeated to obtain multiple layers of MWCNT−AuNP composites.

Biotin−Streptavidin Binding Investigation. The 2D/3D chips were modified by the formation of a self-assembled monolayer (SAM) of 11-amino-1-undecanethiol hydrochloride (11-AUT, Aldrich), which was achieved by incubation of the chips in a 1 mM solution of 11-AUT in ethanol for 1 h at room temperature. The 11-AUT-functionalized chips were then immersed in an ethanol solution containing 0.1 M 1-ethyl-3-[3-(dimethylamino-)propyl]carbodiimide (EDC, Sigma), 0.02 M *N*-hydroxysuccinimide (NHS, Sigma), and 1 mM biotin (Sigma) for 2 h at room temperature, rinsed three times with ethanol, and stored in PBS (0.1 M, pH 7.4) at 4 °C until further use. For the streptavidin binding studies, the biotin-functionalized chips were incubated in 0.7 mL of streptavidin in PBS with a concentration ranging from 0.001 to 100 μg/mL for 1 h. For the real-time binding study, an extinction spectrum was acquired at 550 nm for 2D chips and at 630 nm for 3D chips. The biotin-saturated streptavidin samples were prepared via incubation of a PBS solution with 20 μg/mL streptavidin and 1 mM biotin for 2 h before use.

Antibody−Antigen Binding Investigation. A self-assembled monolayer (SAM) of 11-mercaptoundecanoic acid (11-MUA, Aldrich) was formed on the surface of AuNPs by incubation of the

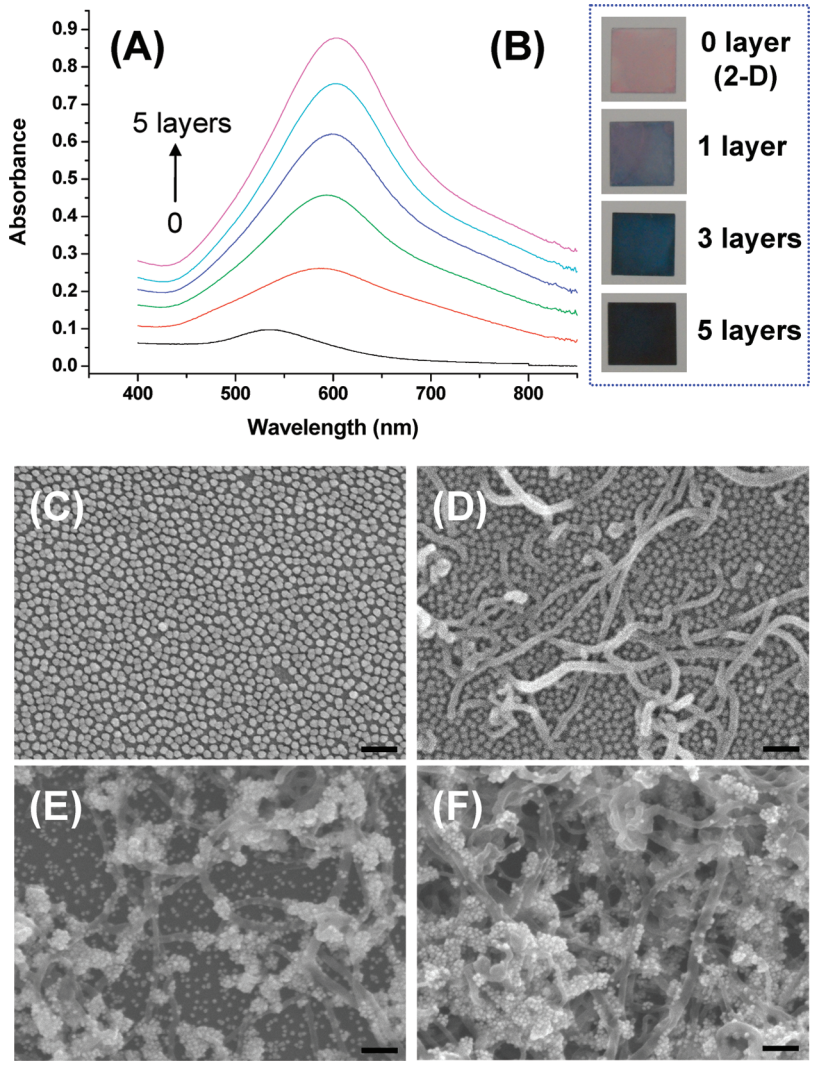

Figure 3. (A) UV−vis absorption spectrum of a self-assembled monolayer of AuNPs, i.e., 2D chip (0 layer, black line) and 3D chips with one to five layers of MWCNT−AuNP composites on glass surfaces. (B) Photos of MWCNT−AuNP chips with different numbers of MWCNT−AuNP layers. The color changes from light pink to dark blue indicate an increasing number of MWCNT−AuNP layers. (C) SEM image of a 2D chip. (D) MWCNTs tethered on AuNPs. (E) One layer of MWCNT with AuNPs on a Si wafer. (F) Five layers of MWCNT with AuNPs on a Si wafer. Note that AuNPs in panels C and D appear to be larger than those in panels E and F because of Pt coating for SEM imaging in panels C and D. The scale bar is 100 nm.

2D/3D chips in a 10 mM solution of 11-MUA in ethanol for 30 min. The SAM was rinsed in ethanol followed by distilled water. The 11-MUA-attached chips were activated for protein immobilization with an aqueous solution containing 0.1 M EDC and 0.02 M NHS for 2 h. Then, the SAMs were incubated in PBS (0.1 M, pH 7.4) containing 2.5 mg/mL HSA (Sigma) for 2 h. The HSA-functionalized glass chips were stored in PBS at 4 °C until further use. Antibody binding events were examined via measurement of the UV−vis absorption spectra of the HSA-functionalized chips before and after incubation in anti-HSA (clone HSA-11, ascites fluid, Sigma) solutions for 1 h.

RESULTS AND DISCUSSION

The overall fabrication procedure of the 3D chip is shown in Figure 1. The procedure includes three main steps: modification of MWCNTs with SH, fabrication of monolayered AuNPs, i.e., 2D chips, and LbL deposition of CNTs/AuNPs. 3-Mercaptopropyltriethoxysilane (MPTES) was adapted to functionalize MWCNTs instead of the conventional aliphatic bifunctional thiols. MPTES is known to undergo self-polymerization in an ethanol solution. Therefore, we hypothesize that a number of SH groups can be introduced by (1) self-polymerization of MPTES after it binds to individual COOH groups in the side wall of MWCNTs, where a relatively small number of COOH groups are available, and/or (2) reaction of MPTES with several COOH groups, e.g., on both ends of MWCNTs, where more COOH groups are available (Figure 2). Such high-density SH groups introduced onto the MWCNT surface allow a number of AuNPs to be immobilized. In parallel, MWCNTs were utilized to provide (1) a large surface area and multiple binding sites within a few steps of modification and (2) microporous structures of multilayered MWCNTs to allow high accessibility of target molecules.

There are two methods that have been widely used for the fabrication of monolayered AuNPs on glass substrates: one that uses silane with a thiol functional group and another that uses

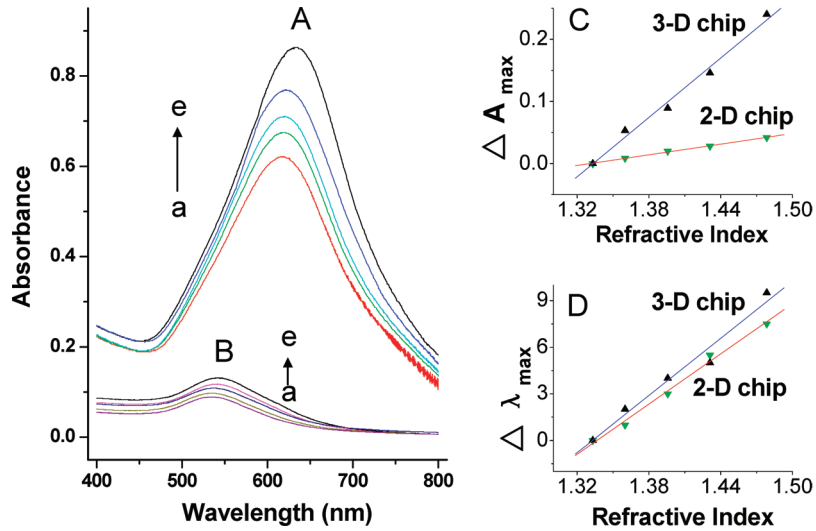

Figure 4. UV−vis absorption spectra of (A) 2D and (B) 3D chips (three layers) in solvents with different RIs: (a) water ($n = 1.33$), (b) ethanol ($n = 1.36$), (c) butanol ($n = 1.3957$), (d) DMF ($n = 1.431$), and (e) DMSO ($n = 1.4785$). Comparison between 2D and 3D chips of the dependence of (C) ΔA_{max} and (D) $\Delta\lambda_{max}$ on the RIs of the surrounding medium.

silane with amino groups. In AuNP conjugation on a glass surface, MPTES was always used for the former method[28,29] and 3-aminopropyltriethoxysilane (APTES) for the latter.[9,10] On the basis of our preliminary results, we adapted APTES for 2D chip fabrication because of its relatively easy chemistry (no need for inert conditions) and better reproducibility, which are consistent with other reports.[11,30]

Figure 3C−F shows the FE-SEM images of the overall steps in the fabrication of the 3D chip. A monolayer of AuNPs is homogeneously distributed on a glass surface, and no aggregation is observed in Figure 3C. Figure 3D shows functionalized MWCNTs tethered on the layer of AuNPs via thiol−Au conjugation. One and five layers of MWCNT−AuNP composites are shown in panels E and F of Figure 3, respectively. Note that panels E and F show 3D chips on electrically conductive Si wafers with the same chemistry and no platinum coating for SEM imaging because the MWCNT−AuNP composites on glass substrates cannot be seen clearly after Pt coating.

The enhancement of sensitivity in 3D chips compared to that in 2D chips was measured on the basis of the extinction spectra of UV−vis absorption (Figure 3A). UV−vis absorption increased dramatically with the number of layers of MWCNT−AuNP composites up to five layers, because of the high density of AuNPs dispersed in each layer of the MWCNTs. The UV−vis absorbance of the five-layer chip was nearly 10 times that of the monolayered AuNP chip. λ_{max}, the wavelength of peak absorbance, was observed to shift from ~530 nm (for the monolayer) to ~600 nm (for five layers) after LbL deposition of MWCNT−AuNP composites, possibly because of the aggregation of some portion of AuNPs during the LbL fabrication.

We examined the ability of the 3D chips to transduce changes in the surrounding medium's RIs into the absorption spectrum. We found that the sensitivity of 3D chips increased with the number of MWCNT−AuNP layers, but the reproducibility was compromised beyond three layers. Three-layer MWCNT−AuNP composites were therefore selected as showing the best balance between sensitivity and reproducibility for 3D chips. Figure 4 shows the absorption spectrum of three-layer 3D chips (A) and 2D chips (B) in different solvents, with refractive indices in the range of 1.333−1.478. Both 3D and 2D chips exhibited a red shift in the peak wavelength, along with an increase in peak intensity as a function of the RIs of the solvent. Panels C and D of Figure 4 show a linear fit for changes in peak absorbance (ΔA_{max}) and peak wavelength ($\Delta\lambda_{max}$), respectively, as a function of the RIs. ΔA_{max} and $\Delta\lambda_{max}$ were 1.5925 AU/RI unit (RIU) and 61.29 nm/RIU, respectively, for the 3D chip but 0.2853 AU/RIU and 53.85 nm/RIU, respectively, for the 2D chip, indicating that the spectral responses of the 3D chip to changes in the surrounding medium's RIs were much superior to those of the 2D chip. Via comparison of the optical behavior of monolayer and multilayer nanoparticle structures, a large change in the RIs in the intensity and only a small change in the RIs in the wavelength likely indicate that the increase in RIs is primarily attributed to the number of particles, while other effects such as interaction between nanoparticles are minimal. On the other hand, changes in ΔA_{max} showed much less batch-to-batch variation than the λ_{max} (data not shown), possibly because of the random distribution and uneven coupling of AuNPs within the multilayer structures.[21] The ΔA_{max} was therefore selected to quantify biomolecule binding on the MWCNT−AuNP composites.

To validate the feasibility of using the 3D chip as a LSPR-based biosensor, biotion and streptavidin were used as model proteins for receptor−analyte binding experiments. A significant increase in the intensity of absorbance was observed in the biotin-functionalized 3D chip after incubation in a series of solutions with different concentrations of streptavidin for 1 h at room temperature. The ΔA_{max} was proportional to the streptavidin concentration, which varied from 0.607 (with control PBS) to 0.725 (100 μg/mL streptavidin), as seen in Figure 5A. Figure 5B represents the time-dependent streptavidin binding on the biotin-functionalized 3D chips, showing that both the binding kinetics and the

(28) Marinakos, S.; Chen, S.; Chilkoti, A. *Anal. Chem.* **2007**, *79*, 5278–5283.
(29) Mayer, K.; Lee, S.; Liao, H.; Rostro, B.; Fuentes, A.; Scully, P.; Nehl, C.; Hafner, J. *ACS Nano* **2008**, *2*, 687–692.
(30) Grabar, K. C.; Freeman, R. G.; Hommer, M. B.; Natan, M. J. *Anal. Chem.* **1995**, *67*, 735–743.

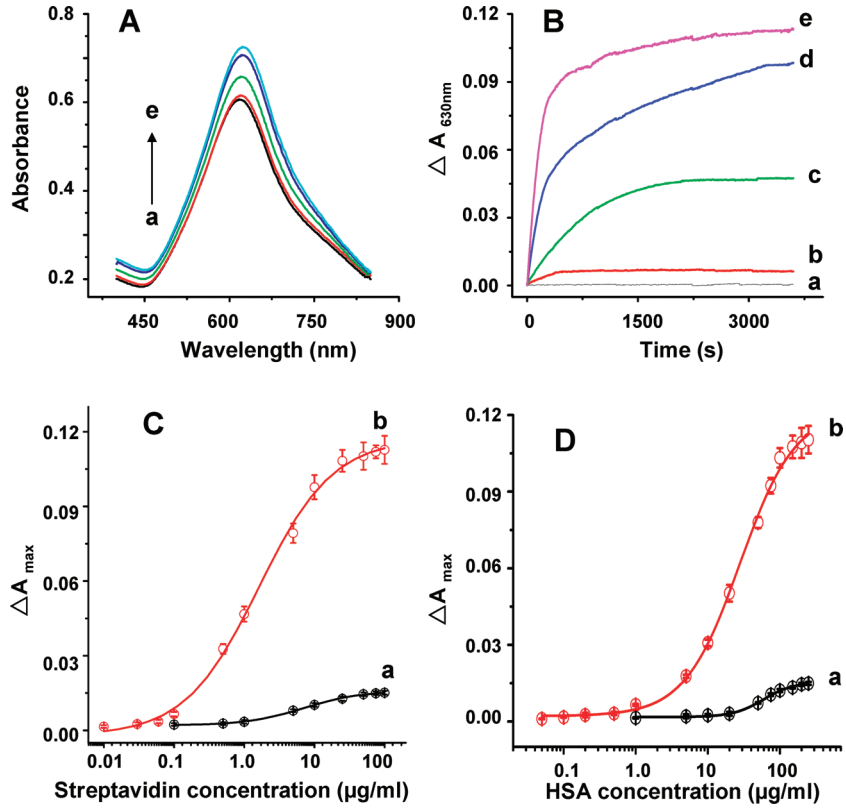

Figure 5. Comparison of 2D and 3D (three layers) chips for receptor-analyte detection. (A) Absorption spectrum of biotin-functionalized 3D chips assayed with streptavidin at (a) 0, (b) 0.1, (c) 1, (d) 10, and (e) 100 μg/mL. (B) Absorbance intensity of biotin-functionalized 3D chips at 630 nm as a function of time in (a) 20 μg/mL biotin-saturated streptavidin, (b) 0.1 μg/mL streptavidin, (c) 1 μg/mL streptavidin, (d) 10 μg/mL streptavidin, and (e) 100 μg/mL streptavidin. (C) ΔA_{max} for biotin-functionalized (a) 2D and (b) 3D chips as a function of streptavidin concentration. (D) ΔA_{max} for HSA-functionalized (a) 2D and (b) 3D chips as a function of anti-HSA concentration. Error bars in panels C and D represent the standard deviation ($n = 3$).

maximum amount of protein bound to the surface at steady state are directly related to the concentrations of biomolecules in a solution. These results are consistent with previous observations.[9,31] A solution of 20 μg/mL biotin-saturated streptavidin was used to validate the specific binding of streptavidin (Figure 5B, a). The absence of changes in absorbance in the biotin-saturated streptavidin solution confirmed that the increase in absorbance upon incubation with streptavidin can be attributed to molecular recognition between streptavidin and biotin tethered to the chip surface.

Figure 5Cb shows a dose−response curve of streptavidin applied to biotin-functionalized MWCNT−AuNP surfaces using ΔA_{max}. A linear rage of 0.1−25 μg/mL with an R^2 of 0.9945 can be estimated from the sigmoidal calibration plot. The corresponding detection limit was estimated to be 0.03 μg/mL (0.5 nM), based on a signal-to-noise ratio (S/N) of 3. The dose−response curve of the 2D chip is also plotted in Figure 5Ca for direct comparison with that of the 3D chip. A dynamic range of 1.0−50 μg/mL and a detection limit of 0.6 μg/mL (10 nM) were estimated for the 2D chip. Overall, 3D chips exhibited a wider dynamic range and a 20-fold lower detection limit than the 2D chips.

The 3D chips as LSPR-based biosensors were further validated by HSA and its antibody. Figure 5D shows the dose−response curves of ΔA_{max} as a function of anti-HSA concentration for HSA-functionalized 2D and 3D chips. The corresponding detection limits were estimated to be 10 μg/mL (~66.7 nM) and 0.5 μg/mL (~3.33 nM) for the 2D and 3D chips (based on a S/N of 3), respectively. The low sensitivity of anti-HSA detection compared to that of streptavidin could mainly be attributed to the different affinity of the binding pairs as the dissociation constants for the streptavidin−biotin and HSA−anti-HSA complexes were reported to be 10^{-15} and ~10^{-9} M, respectively.[32]

CONCLUSIONS

In conclusion, we reported a novel method for the fabrication of three-dimensionally assembled AuNP films by LbL deposition of MWCNTs for the application of highly sensitive plasmonic biosensors in conventional UV−vis instruments. Some original and important findings of this study are as follows. (1) Highly dense and accessible AuNPs were created by the introduction of multiple SH groups onto MWCNT surfaces. (2) The fabrication of 3D chips can be easily accomplished by repeated dipping of substrates into a MWCNT-Si-SH solution followed by a AuNP solution. (3) Compared to 2D chips, 3D chips exhibited a 5.6-fold better spectral response in bulk refractive index change, resulting in an ~20-fold higher sensitivity and wider dynamic range in biotin−streptavidin and HSA−anti-HSA recognition. This 3D chip has many potential applications in microarray-based LSPR sensors,

(31) Andrade, J. D.; Hlady, V. *Protein adsorption and materials biocompatibility: A tutorial review and suggested hypotheses*; Springer: Berlin, 1986.

(32) Nisonoff, A. *Introduction to Molecular Immunology*, 2nd ed.; Sinauer Associates, Inc.: Sunderland, MA, 1984.

in which the LSPR signal is often weak because of the low density of nanostructures in the defined surface areas.

ACKNOWLEDGMENT

This research was supported by a grant to D.-H.K. from the Academic Research Funding Tier 1 (RG65/08) and the National Medical Research Council (NMRC/NIG/00602009) of Singapore. G.C. acknowledges the National Nature Sciences Foundation of China (20735002 and 20877019).

Received for review February 7, 2010. Accepted May 2, 2010.

AC100346Z